

# Assessment of dissipated energy-based failure criteria for sands under cyclic loading

Evaluación de criterios de falla basados en energía disipada para arenas bajo cargas cíclicas

## Guillermo J. Zavala, Ph.D., P.E.

Soil Mechanics Laboratory, Pontificia Universidad Católica del Perú, Perú, gzavala@pucp.edu.pe

Miguel A. Pando, Ph.D., P.Eng.

Civil, Architectural and Environmental Engineering Department, Drexel University, Philadelphia, PA, USA

Youngjin Park, Ph.D.

Energy Production and Infrastructure Center, University of North Carolina at Charlotte, Charlotte, NC, USA

Rafael Aguilar, Ph.D.

Department of Engineering, Pontificia Universidad Católica del Perú, Perú

ABSTRACT: There are many criteria proposed by the geotechnical community to define the failure of sands under cyclic loading. The three main categories of these failure criteria are: i) shear strain-based, ii) effective stress equal zero (excess pore water pressure-based (for saturated sands), and iii) strength-based. A comprehensive laboratory study by the authors involving over 262 constant volume cyclic simple shear (CSS) tests on dry Ottawa sand samples prepared at different initial states and subjected to different cyclic load waveforms, and frequencies allowed the comparison of the cumulative dissipated energy to failure using different classical failure criteria. This paper also presents three alternative failure criteria based on the plots of cumulative dissipated energy versus load cycles and the location where the sample starts to experience a sudden increase in energy dissipation rate. The results indicate that the cumulative dissipated energy can be an adequate early predictor of failure as the amount and rate of dissipated energy start to increase drastically at the onset of failure.

KEYWORDS: cyclic behavior, failure criteria, dissipated energy to failure; cyclic simple shear; irregular cyclic loading.

## 1 INTRODUCTION

The behavior of sands under cyclic loading is relevant to performance during earthquakes, machine loading, and other sources of dynamic cyclic loading. Many of these situations can involve complex time histories of cyclic loading, resulting in large shear strain levels leading to failure. If the sand is initially saturated, and the cyclic loading is fast enough to have undrained conditions, the soil may develop significant excess pore water pressures that can lead to cyclic liquefaction. Over the years, many criteria have been proposed by the geotechnical community to define the failure of sands under cyclic loading. The three main categories of failure criteria for sands under cyclic loading are: i) shear strain-based, ii) excess pore water pressure-based (used for saturated sands and commonly used for liquefaction) or zero effective stress-based (for both dry and saturated sands), and iii) strength-based. As illustrated in the examples presented in this paper, the various definitions will predict failures at different instances of the tests, as they are based on different factors. The occurrence of the different failure criteria varies significantly depending on the initial state of the sample that in critical state soil mechanics (e.g., Schofield and Wroth 1968) can be defined by the initial values of the sample relative density and effective vertical stress level.

In this paper, the authors compare different existing failure criteria using a comprehensive laboratory study reported by Zavala

et al. (2022a). The main objectives of this work are to: 1) Quantify the progression of energy dissipation in a cyclic simple shear (CSS) test with varying initial conditions and applied loading conditions until failure 2) Characterize the relationship between different test parameters such as Double Amplitude (DA) strain and effective stress, and the cumulative dissipated energy during CSS tests, and 3) Investigate the relationship between the different failure criteria and the cumulative dissipated energy. This paper proposes alternative failure criteria based on sudden changes in the cumulative dissipated energy experienced by the laboratory sample during cyclic loading. The results indicate that the cumulative dissipated energy can be an adequate predictor of failure, particularly as an early predictor, as the amount and rate of dissipated energy increases drastically at the onset of failure.

## 2 CLASSICAL FAILURE CRITERIA

As mentioned above, the three main categories to define failure for sands under cyclic loading used in the academic community and in engineering practice are based on: i) shear strain, ii) excess pore water pressure (used for saturated sands and commonly used for liquefaction) or zero effective stress (for both dry and saturated sands), and iii) strength. This section describes the commonly used criteria under these three categories.



#### 2.1 Strain-based criteria

This group of failure criteria defines failure as a sand sample under cyclic loading reaching a prescribed level of shear strain or deformation. Strain-based failure criteria are commonly used for liquefaction studies.

Due to the strong correlation between the seismic performance of sands and structures built over or out of them, shear strain and deformation of the sands have been reported to serve as a good criterion for seismic performance assessment (Wu et al. 2004). A drawback of this type of failure criteria is the variation of the selected level of strain used to define failure. Different researchers have used levels between 2% and 10%. For liquefaction, for example, the selection of strain level used to define the onset of liquefaction varies significantly based on the author and the type of laboratory testing used. Ishihara (1985) proposed defining liquefaction 3% single amplitude (SA) strain as a criterion to define liquefaction in simple shear tests and in field studies with level ground conditions. Ishihara (1996) proposed defining liquefaction when the sample reached 5% double amplitude (DA) of axial strain in cyclic triaxial testing. The selection of the strain level varies based on the initial relative density, i.e. loose to dense, of the test sample (Wu et al., 2004). In this paper involving CV-CSS testing we considered the strain-based failure criteria of 6% and 7.5% DA of shear strain.

#### 2.2 Pore pressure (or zero effective stress level) based criteria

This failure criterion defines failure when a sand sample under cyclic loading reaches an effective stress level of zero. For saturated samples under undrained cyclic loading, this is related to a state when the sample develops an excess pore water pressure equal to the initial effective minor principal stress (σ'<sub>30</sub>). For saturated samples, this criterion often uses the pore pressure ratio (r<sub>u</sub>), and failure is defined when this ratio reaches unity (r<sub>u</sub>=1). In loose soils, the r<sub>u</sub>=1 condition is immediately accompanied by large shear strains, but for dense sands, achieving full pore pressure ratio of unity cannot be achieved (Wu et al. 2004). For dry sands, under CV-DSS this criterion would correspond to the state where the applied vertical normal stress reaches zero while maintaining the constant volume condition.

#### 2.3 Strength based criteria

Sands under earthquake loading can experience a sudden strength loss that can trigger failure of structures such as slopes and earth embankments. This failure criterion defines failure when a sand sample under undrained cyclic loading exhibits a sudden strength loss and reaches a residual shear strength at large strains (NASEM 2016). This residual shear strength is often associated to the sample reaching the steady state, thus is referred to the undrained steady state shear strength. Laboratory testing has been used to estimate the undrained steady state shear strength of sands (e.g., Poulos et al. 1985, Yoshimine and Ishihara 1998, Stark et al. 1999), however due scale effects lab testing is generally viewed as unable to replicate the residual shear strength of liquefiable soil in the field (NASEM 2016).

## 3 LABORATORY TESTING PROGRAM

The failure criteria were compared using the results of a comprehensive experimental program performed by the authors (Zavala et al. 2022a) that involved 262 cyclic simple shear (CSS) tests conducted using an Advanced Dynamic Cyclic Simple Shear machine (ADVDCSS) manufactured by GDS Instruments. This experimental program involved constant volume (CV) CSS tests (Figure 1) on uniform dry sand samples prepared at nine different initial states subjected to a wide range of cyclic loading types (e.g., uniform, periodic, non-periodic, and complex irregular earthquake loading). The findings reported using the data from this experimental program supported the notion that specific dissipated energy could be used as a reasonable predictor of failure for uniform sands, based in their initial state (Zavala et al. 2022a). Further research by the same authors provided a simplified approach that can predict failure of dry sands under general shear stress-time histories, based on tests with uniform sinusoidal loading (Zavala et al. 2022b).

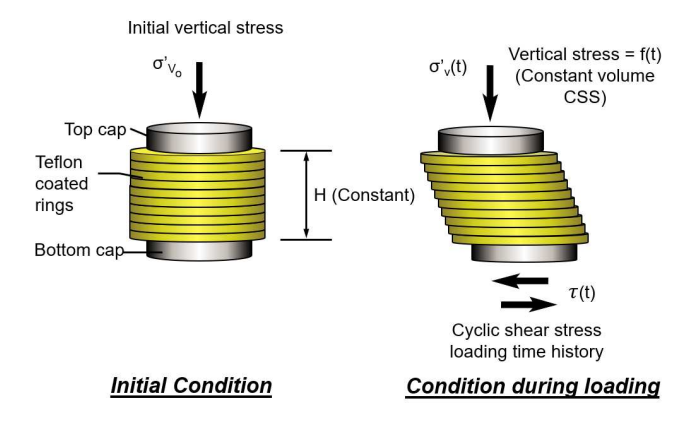


Figure 1. Schematic of a CV-CSS test (Zavala et al. 2022b)

The test sand used in this experimental program was Ottawa 20/30 silica sand, a uniform, poorly graded silica sand with subrounded to rounded grains. The mean particle size ( $D_{50}$ ) of this sand is 0.71 mm, and the 20/30 designation is based on having 95 % retained between the ASTM standard sieves #20 and #30. The maximum and minimum void ratios were measured using laboratory procedures in general accordance with ASTM Standard D4253 (ASTM 2016a) and D4254 (ASTM 2016b), respectively. The average maximum and minimum void ratio values obtained for the test sand were 0.644 and 0.503, respectively. The CV CSS tests were performed using dry Ottawa sand samples prepared at nine initial states corresponding to three different levels of relative density and three initial vertical stress levels as shown in Table 1.

Figure 2 presents the results of one of the CV-CSS tests reported in the experimental program by Zavala et al. (2022a), which is summarized in Table 1. The results correspond to the CV CSS test of a very dense sand ( $D_r = 95\%$ ), initial vertical stress  $\sigma'_{vo}$ =200 kPa, subjected to harmonic (uniform) loading with a cyclic stress ratio (CSR) of 0.065 and a frequency of 0.1 Hz, and are presented using a four-way graph that is typically used to show CSS results.



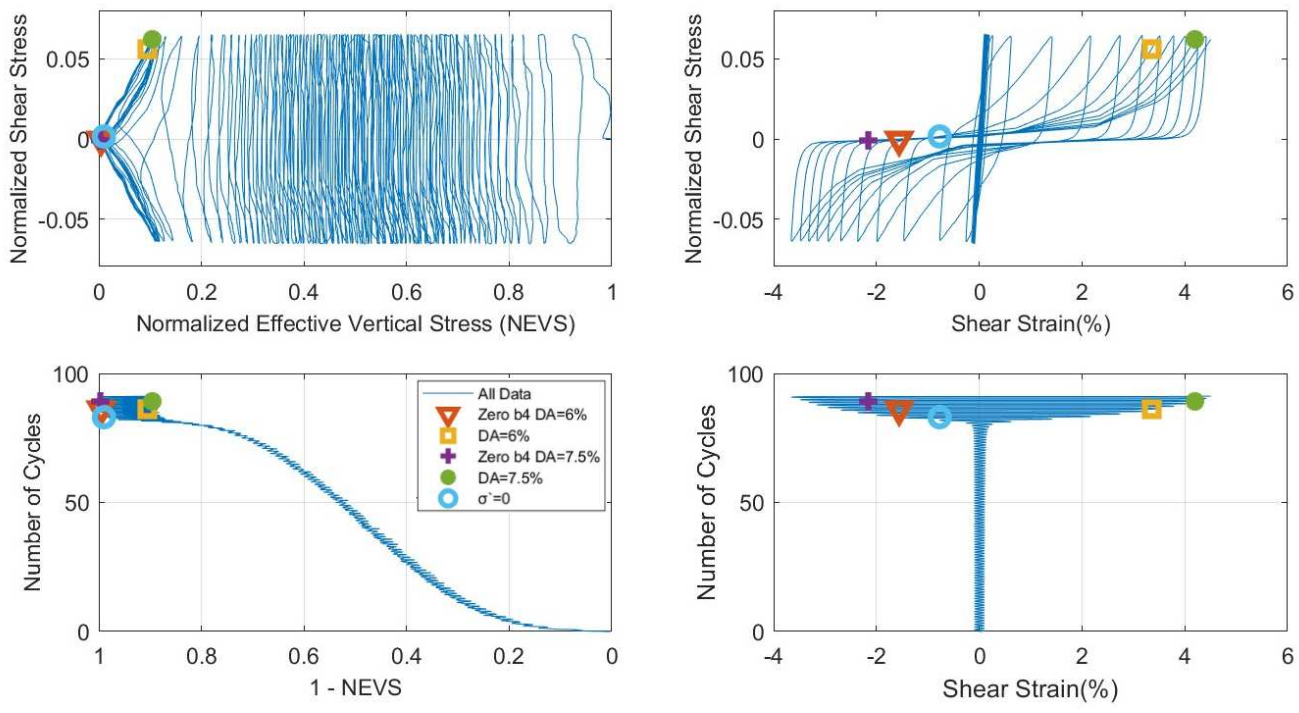


Figure 2. Four-way graph for very dense sand ( $D_r = 95\%$ ),  $\sigma'_{vo} = 200$  kPa, subjected to CSR = 0.065 at 0.1 Hz

| Table 1. Details of the test progr | m by Zavala et al. (2022a) |
|------------------------------------|----------------------------|
|------------------------------------|----------------------------|

| Table 1. Details of the test program by Zavaia et al. (2022a) |   |
|---|---|
| Item  | Details   |
| DESCRIPTION<br>OF TEST<br>SAND                                | Ottawa 20/30 sand Shape: subrounded to rounded $G_s = 2.65$ $D_{50} = 0.71$ mm $C_u = 1.2$ $e_{max} = 0.644$ $e_{min} = 0.503$  |
| INITIAL STATES  | Nine initial states<br>Three $D_r$ from 23% to 100%<br>$\sigma'_{v0} = 100, 200$ , and 400 kPa  |
| TEST PROGRAM<br>(# of tests, loading<br>Types)                | Total number of tests: 262  • 85 uniform tests  - CSR: 0.05 to 0.12  - f = 0.1, 0.5 and 1Hz  • 173 non-uniform tests  4 types of loading  • 4 tests with earthquake signals |

In this type of graph, the CSS test results are presented using 4 plots that have matching axes in the vertical and horizontal directions and are plotted in the same scales. The graph in the upper left shows the Normalized Effective Vertical Stress (NEVS), which is defined as the ratio between the actual vertical stress at any instance in the test and the initial vertical stress applied to the sample at the beginning of the dynamic shearing stage of the test, versus the normalized shear stress  $(\tau/\sigma^{\prime}_{vo})$ . At the beginning of a test the

sample has an NEVS of 1, and as the cyclic shearing progresses, the NEVS value starts to decrease until approaching a value of zero at failure (failure criterion described in 2.2). The value of NEVS decreases because the applied normal stress decreases during loading to ensure that the testing condition of constant sample height (i.e., constant volume) is maintained. This graph illustrates the progressive decrease of the vertical stress with number of applied cycles. When the sample approaches a NEVS value of 0, the shear strains start to increase dramatically which each additional cycle of load applied to the sample and the hysteresis loops and associated dissipated energy tend to increase in magnitude. The graph in the upper right shows the shear strain vs the normalized shear stress  $(\tau/\sigma'_{vo})$ , illustrating the progression in size of hysteresis loops and increase of shear strain levels as the applied load cycles increase. The plot in the lower right shows the variation of shear strain with number of simple shear load cycles. This graph effectively illustrates the number of cycles for which the shear strains start to increase dramatically. Closing, the plot in the lower left corner shows the complement to NEVS, defined as 1 - NEVS, versus the number of applied load cycles.

Figure 2 shows symbols corresponding to two strain-based failure criteria considered (i.e., DA=6% and DA=7.5%) and the effective vertical stress =0 (r<sub>u</sub>=1 for saturated tests). For the two strain-based failure criteria, the points of occurrence were marked when the DA strain occurred and also at points adjusted slightly to correspond to the point of zero shear stress just before the DA level was achieved. Therefore, there are five symbols shown in Figure 1, corresponding to DA=6%, the point of zero shear stress just before DA=6%, DA=7.5%, the point of zero shear stress just before DA=7.5%, and the point of zero vertical effective stress



 $(\sigma'_v)$ . It can be seen from this figure that the different failure criteria occur at different points. In the following section, we will compare the dissipated energy levels of the different criteria.

## 4 DISSIPATED ENERGY CURVES

Using energy-based approaches to study the behavior of soils under cyclic loading is an approach that has gained popularity in recent years. Energy-based approaches are based on comparing the energy associated with the cyclic loading (such as in an earthquake) to the soil resistance expressed in terms of energy. There have been experimental studies investigating the failure of sands under cyclic (primarily liquefaction) as a function of the experienced dissipated energy by the sample (e.g., Nemat-Nasser and Shokooh 1979, Davis and Berrill 1982, Berrill and Davis 1985, Yanagisawa and Sugano 1994, Liang 1995, Green et al., 2000, Polito et al. 2008, Polito et al. 2013, Green and Terri 2005, Lasley 2015, Lasley et al. 2016, Kokusho and Mimori 2015, Azeiteiro et al. 2017, Kokusho 2017, Fardad Amini and Noorzad 2018, Kokusho and Kaneko 2018, Zavala et al. 2022a).

The cumulative dissipated energy per unit volume of a sample subjected to cyclic loading in a CV-CSS test can be obtained from the sum of the hysteresis loops of a plot of shear stress versus shear strain cycles, as shown in Figure 3, as the shaded area for the ith stress-controlled sinusoidal shear stress load cycle of a CSS test. The CV-CSS tests by Zavala et al. (2022a) were run under constant volume conditions and under stress-controlled cycles and typically showed small energy dissipation for the initial stress-strain cycles and increased energy dissipation as the number of load cycles increased. The cumulative specific dissipated energy to failure (E<sub>f</sub>) is computed by adding the different hysteresis loop areas ( $\Delta W_i$ ) of the successive load cycles until sample failure is reached. A detailed description of the procedure used to compute the cumulative specific dissipated energy to failure (E<sub>f</sub>) for CV-CSS tests under uniform or irregular shear stress time histories can be found in Zavala et al. (2022a).

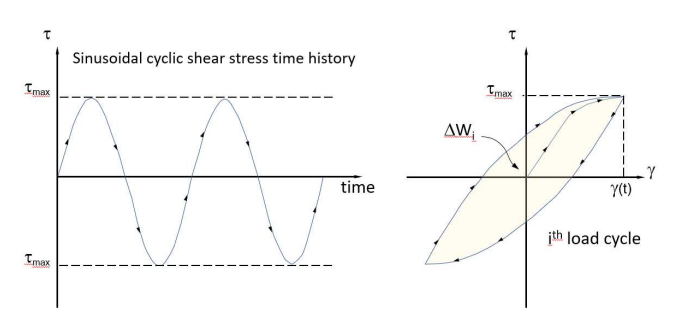


Figure 3. Dissipated energy ( $\Delta W_i$ ) in the  $i^{th}$  load cycle in a CV stress-controlled CSS test under sinusoidal cyclic loading (Zavala et al, 2022b)

Figure 4 shows plots of cumulative dissipated energy for CV-CSS tests from Zavala et al. (2022a). For the sake of brevity, we only show a set of tests corresponding to Ottawa sand samples prepared at nine initial states all tested with a sinusoidal loading with a CSR equal to 0.065 and a frequency of 0.1 Hz. The nine plots present the progression of cumulative dissipated energy vs number of cycles corresponding to the none initial states corresponding to three relative density levels (loose, dense, and very dense) and for the three initial levels of vertical effective stress

considered in the study (i.e., 100, 200, and 400 kPa). All plots show five symbols to denote the location when the different failure criteria described above were achieved (note that the legend is shown inside the upper left plot). In other words, the five symbols correspond to DA strain=6%, the point of zero shear stress just before DA strain=6%, DA strain=7.5%, the point of zero shear stress just before DA=7.5%, and zero vertical effective stress (i.e., NEVS = 0). Each of the nine plots includes a summary table summarizing the coordinates (i.e., the cycle number and the cumulative dissipated energy) where each failure criterion occurs.

Regarding the general shape of the plots of cumulative dissipated energy versus the number of cycles, as shown in Figure 4, all tests showed an initial straight portion of the cumulative dissipated energy graph, followed by a transition curve where a distinct increase of the rate of energy dissipation is observed, followed by a second relatively straight portion with a more pronounced slope corresponding to the increased rate of dissipation. Figure 4 shows that all of the traditional failure criteria occurred within the second linear portion of the graphs.

The data set in Figure 4, as well as other similar test sets by the Zavala et al. (2022b), shows that for a given CSR value, the number of cycles required to reach the transition region of increasing dissipation rate will depend on the sample initial relative density and vertical stress level. In general, a higher relative density and a higher initial vertical stress will require more cycles to reach the second linear region with a higher slope. However, as shown in Figure 4, the amount of cumulative dissipated energy at the transition point was found to be more sensitive to the initial vertical stress level and, to a lesser extent, to the relative density of the sample. The values of cumulative dissipated energy of the transition points shown in Figure 4 increase with increasing levels of the initial vertical stress. Furthermore, by comparing plots in Figure 4 with the same level of initial vertical stress, it can be noted that the relative density of the soil has very little effect on the dissipated energy required to reach the effective stress zero failure criterion (even though, as explained before, the number of cycles to reach that criterion is much higher). However, the initial relative density of the sample does have a significant effect on the cumulative dissipated energy values required to reach either of the two DA strain criteria considered.

In very dense samples, the order of occurrence of the classical failure criteria was the same for all stress levels: all tests on very dense samples reached first the effective vertical stress equal zero  $(\sigma'_{v}=0)$ , followed by both DA strain criteria. For the tests on dense samples, the occurrence of the different failure criteria also occurred in the same order as for very dense samples for all stress levels, but the locations of the failure points in the cumulative dissipated energy plots criteria are closer. Finally, for tests on loose samples, the different failure criteria tend to occur very close to each other and often in the same load cycle, thus the order of occurrence of the different criteria varied, and in some cases even occurred in the reverse order compared to the other relative densities, where the location of the DA strain=6% and DA strain=7.5% even occurred before the effective stress reached zero. This reverse order was observed particularly for tests at higher levels of initial effective stress.

Comparison plots of the cumulative specific dissipated energy required to reach the different failure criteria is shown in Figure 5, for the three relative densities considered in this study.

Proceedings of the 17<sup>th</sup> Pan-American Conference on Soil Mechanics and Geotechnical Engineering (XVII PCSMGE), and 2<sup>nd</sup> Latin-American Regional Conference of the International Association for Engineering Geology and the Environment (IAEG), La Serena Chile, 2024.

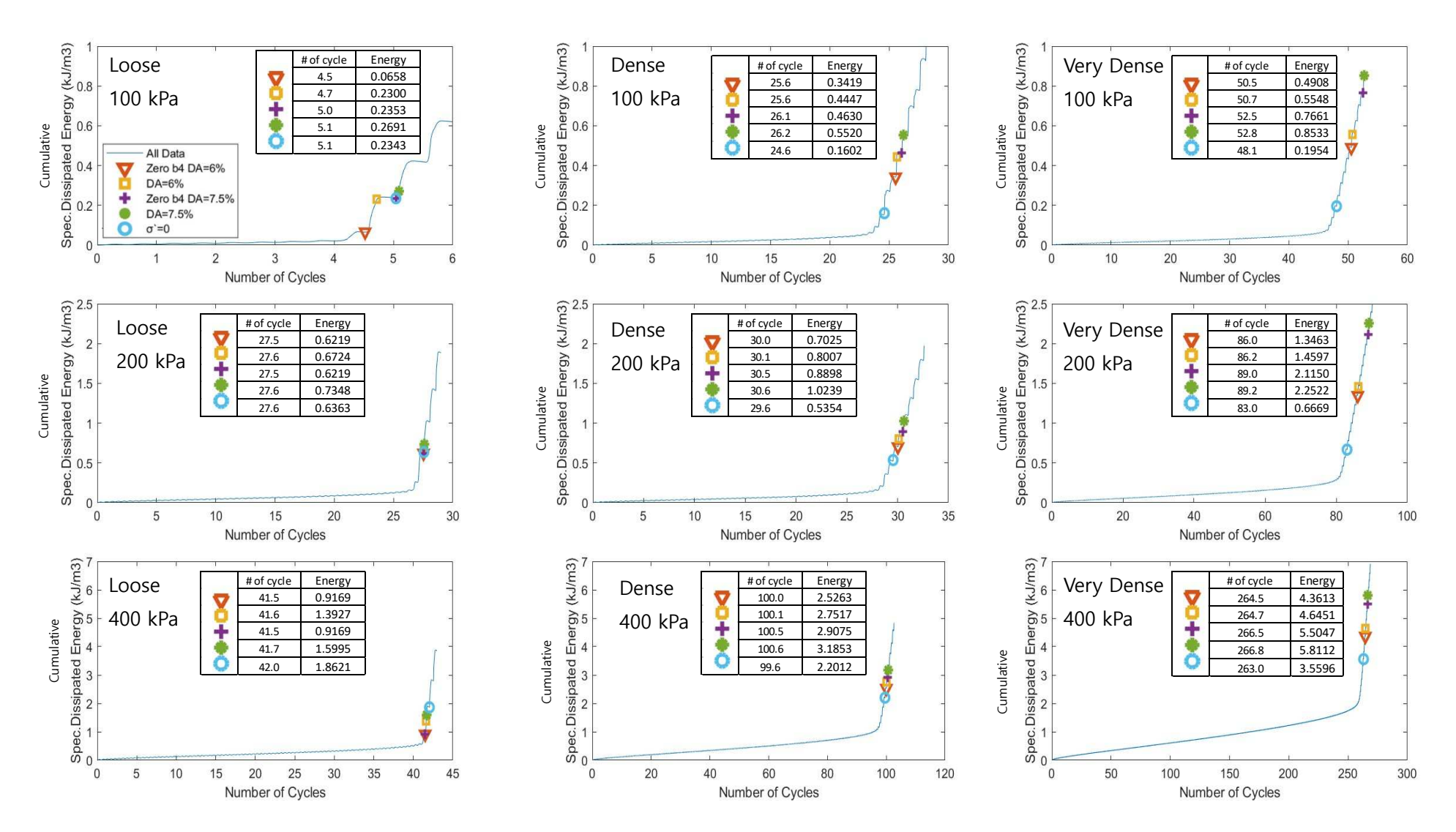
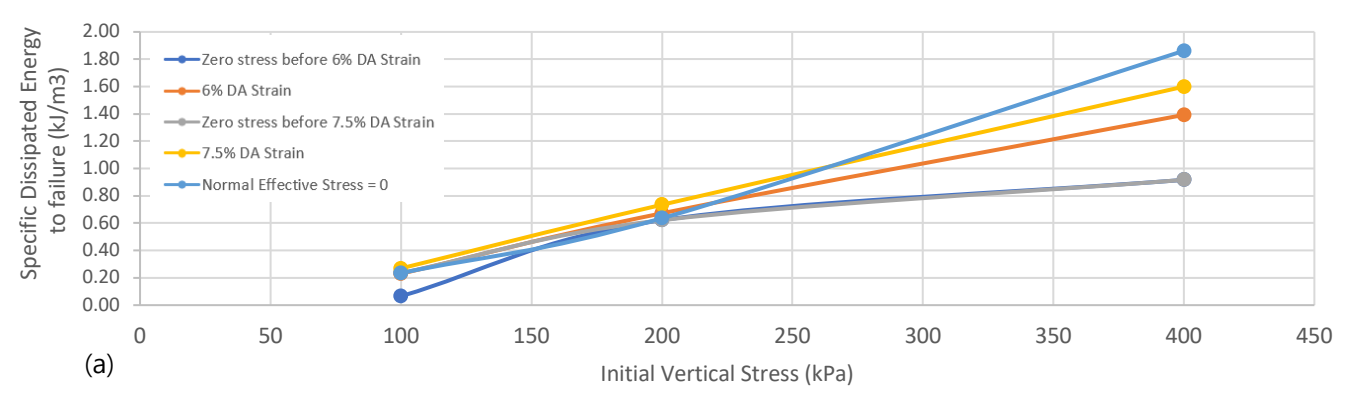


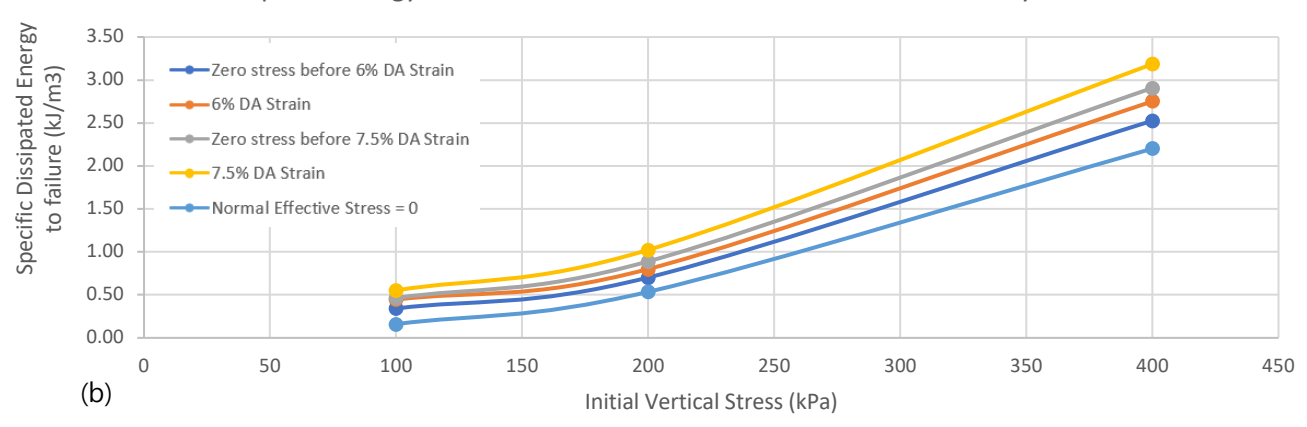
Figure 4. Cumulative dissipated energy versus load cycle for CV-CSS tests from Zavala et al. (2022) with sinusoidal loading with a CSR equal to 0.065 and a frequency of 0.1 Hz



# Dissipated Energy for different failure criteria - Initial Relative Density = 29%



# Dissipated Energy for different failure criteria - Initial Relative Density = 67%



# Dissipated Energy for different failure criteria - Initial Relative Density = 97%

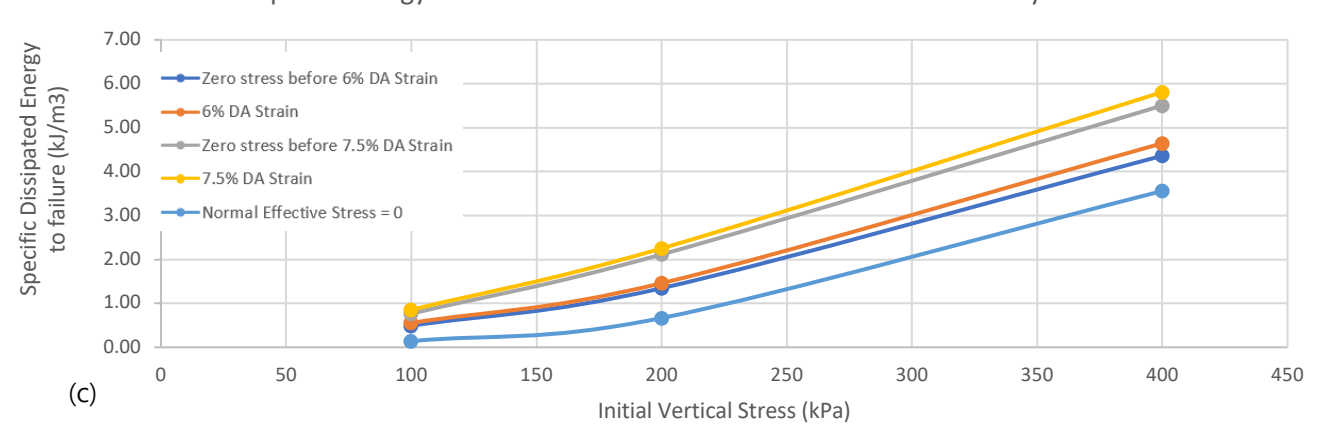


Figure 5. Comparison of cumulative specific dissipated energy values as a function of level of initial vertical stress, for the different failure criteria and the 3 relative densities: (a) Loose (Ave. D.=29%) (b) Dense (Ave. D.=67%) and (c) Very Dense (Ave. D.=97%)



Figure 5 illustrates the earlier observations regarding the order of occurrence of the points using the different classical failure criteria considered. The plots in this figure show that the value of cumulative dissipated energy required to reach the different failure points increases with increasing initial vertical stress. Also, for the dense and very dense samples, the order of occurrence of traditional failure criteria is unaffected by the level of initial vertical stress, with the effective vertical stress equal to zero occurring first, followed by the occurrence of the two strain failure criteria. In contrast, as mentioned earlier, for loose samples the order of occurrence was not constant. For the tests on loose samples, the order of occurrence was even reversed in some cases, particularly for the tests performed at high initial vertical stresses.

## 5 DISSIPATED ENERGY-BASED FAILURE CRITERIA

### 5.1 Description of dissipated energy-based failure criteria

As mentioned in the previous section, the plots of cumulative dissipated energy versus applied load cycles (or time of loading), like the ones shown in Figure 4, show that the traditional failure criteria based on strain level or effective stress equal zero, occur at different levels of cumulative dissipated energy. Furthermore, these curves of cumulative dissipated versus number of cycles (or time of loading) typically have an initial portion where the dissipated energy dissipates at a gradual and slow rate that can be approximated with a straight line. Then, as the sample gets closer to failure, it transitions into a faster rate of dissipation that can also be approximated to a straight line with a steeper slope than the initial stage. These two linear regions (≈ "straight lines") are connected by a curved transition zone. As discussed in Section 4, all traditional failure criteria were found to fall on the second linear portion with a steeper slope that corresponds to a faster rate of energy dissipation.

Based on the observed general bilinear shape of these plots of cumulative dissipated energy vs number of applied load cycles (or time), it is possible to define three energy-based failure criteria as shown schematically in Figure 6. The plot shows two dashed lines corresponding to a linear regression to the two linear regions of the cumulative dissipated energy plots. Criteria 1 and 2 correspond to the points where the experimental curve separates from the linear regression, and the point corresponding to Criterion 3 is obtained from the intersection of the two linear regression lines.

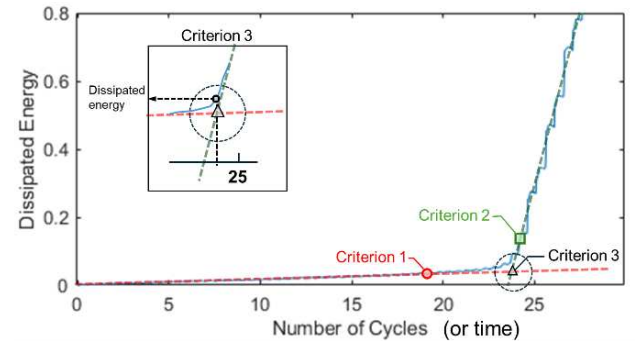


Figure 6: Possible alternatives for energy-based failure criteria

The three energy-based failure criteria shown in Figure 6 correspond to: 1) point in the curve where the dissipated energy plot departs from a best fit linear regression in the first linear branch (Criterion 1). 2) the first point of the plot that intersects the linear regression of the second linear branch of the curve (Criterion 2), and 3) the intersection of the lines fitted to the two straight portions of the curve (Criterion 3). For this third criterion, the inset in Figure 6 shows how the dissipated energy can be obtained by plotting the vertical line up to the dissipated energy plot.

These three energy-based failure criteria occur before the classical failure criteria, and thus could serve as an early warning of the onset of failure of a test as they are located just before or at the beginning of the second straight-line portion of these types of plots.

#### 5.2 Comparison of dissipated energy-based failure criteria

This subsection compares the three dissipated energy-based failure criteria described above, with the commonly used traditional failure criteria described in Section 2. For the sake of brevity, we present this comparison for the CV-CSS test with uniform sinusoidal loading (CSR = 0.065) on a very dense sand subjected to an initial vertical stress of 100 kPa reported by Zavala et al. (2022a). The plot of cumulative dissipated energy for this test was presented in the top right corner of Figure 4 and is presented again in Figure 7 with the addition of the three possible dissipated energy-based criteria.

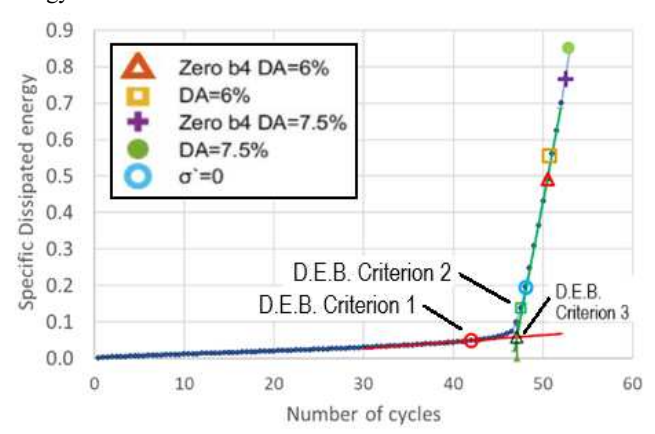


Figure 7: Comparison of three proposed dissipated energy-based (D.E.B.) criteria (Criteria 1, 2, and 3) with traditional failure criteria for a CV-CSS test with a CSR= 0.065 on a very dense sand at 100 kPa.

Figure 7 shows that Criterion 1 occurs at approximately after 42 load cycles and a specific accumulated dissipated energy of 0.0483 kJ/m³. Criterion 2 occurs approximately after 47.5 load cycles and at 0.1374 kJ/m³ of specific cumulative dissipated energy, and Criterion 3 occurs at approximately 46.8 cycles and at 0.0992 kJ/m³ of specific cumulative dissipated energy. In contrast, the traditional failure criteria all occur after dissipated energy-based Criterion 2, and further up the second linear region of the dissipation curve. The first traditional failure criterion (σ'=0) occurs after 48.1 load cycles and at a specific cumulative dissipated energy of 0.1954 kJ/m³. Both strain-based failure criteria occur at a higher number of cycles and cumulative dissipated energy. The early occurrence of the dissipated energy-based failure criteria was observed for all other tests reported by Zavala et al. (2022a).



Proceedings of the 17<sup>th</sup> Pan-American Conference on Soil Mechanics and Geotechnical Engineering (XVII PCSMGE), and 2<sup>nd</sup> Latin-American Regional Conference of the International Association for Engineering Geology and the Environment (IAEG), La Serena Chile, 2024.

Therefore, any of the three proposed dissipated energy-based criteria can help identify when a rapid rate of change of the dissipated energy has started or is about to occur. Thus, the three possible energy-based criteria could potentially serve as an early warning of the onset of failure of the sample. However, more research in this area, looking at different sands and more types of testing, is recommended to confirm and extend these findings.

## 6 CONCLUSIONS

This study used the results of a comprehensive laboratory study by the authors (Zavala et al. 2022b) that involved over 262 CV- CSS tests on dry Ottawa sand samples prepared at nine different initial states and subjected to different cyclic load waveforms to investigate the progression of energy dissipation from start to failure. The paper compares the cumulative specific dissipated energy levels observed in this experimental program for different classical failure criteria commonly used in research and in practice. The paper presents three alternative failure criteria based on sudden changes in the plots of cumulative dissipated energy versus load cycles and the results indicate that the three cumulative dissipated energy-based failure criteria used could be an adequate early predictor of failure as the amount and rate of dissipated energy start to increase drastically at the onset of failure.

The main conclusions drawn from this study are:

- All tests analyzed showed a distinct change in the rate of cumulative energy dissipation after a certain number of cycles, which increases with higher relative density and higher initial vertical stress.
- The location of all traditional failure criteria occurred in the second linear branch of the cumulative dissipated energy versus load cycle curves.
- The value of cumulative dissipated energy required to reach the transition zone, i.e., where the rate of energy dissipation increases, was found to mostly depend on the level of initial vertical stress and to a lesser extent on the relative density of the sample.
- For dense and very dense samples, the failure criterion based on vertical effective stress = 0 occurred before the strain-based failure criteria; for loose samples, this was not always the case as in some instances, the strain-based criteria occurred first
- For a given level of initial vertical stress, the locations of the traditional failure criteria were close to each other for the loose samples, and this spacing increased with increasing relative density.
- The relative density of the soil has almost no effect on the value of cumulative dissipated energy required to reach the effective stress zero failure criterion. In contrast, relative density was found to have a significant effect on the dissipated energy required to reach either of the strain-based failure criteria.
- Three dissipated energy-based failure criteria were proposed, which were found to always occur before the traditional failure criteria. Thus, they could serve as an early warning for the onset of failure of a sample of sand subjected to cyclic loading.

## 7 ACKNOWLEDGEMENTS

The authors would like to thank Pontificia Universidad Católica del Perú for funding the first author's completion of the experimental program. The first author also thanks the second author for hosting him and providing access to the required testing and computing facilities.

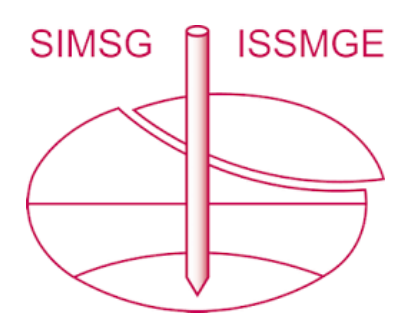
#### 8 REFERENCES

- ASTM. 2016a. ASTM D4253 Standard Test Methods for Maximum Index Density and Unit Weight of Soils Using a Vibratory Table. ASTM International, West Conshohocken, PA, USA, DOI: 10.1520/D4253-16F01.
- ASTM 2016b. ASTM D4254 Standard Test Methods for Minimum Index Density and Unit Weight of Soils and Calculation of Relative Density. ASTM International, West Conshohocken, PA, USA, DOI: 10.1520/D4254-16.
- Azeiteiro R.J.N., Coelho P.A.L.F., Taborda D.M.G., and Grazina J.C.D. 2017. Energy-based evaluation of liquefaction potential under nonuniform cyclic loading. *Soil Dynamics and Earthquake Engineering*, 92, 650-665, DOI: 10.1016/j.soildyn.2016.11.005
- Berrill J.B., and Davis R.O. 1985. Energy dissipation and seismic liquefaction of sands: Revised model. *Soils and Foundations* 25(2), 106–118
- Davis R.O. and Berrill J.B. 1982. Energy dissipation and seismic liquefaction in sands. Earthquake Engineering and Structural Dynamics 10, 59–68.
- Fardad Amini P. and Noorzad R. 2018. Energy-based evaluation of liquefaction of fiber-reinforced sand using cyclic triaxial testing. Soil Dynamics and Earthquake Engineering 104, January 2018, 45–53. https://doi.org/10.1016/j.soildyn.2017.09.026
- Green R.A., and Terri, G.A. (2005). Number of equivalent cycles concept for liquefaction evaluations - Revisited. ASCE Journal of Geotechnical and Geoenvironmental Engineering 131(4), 477–488.
- Green R.A., Mitchell J.K., and Polito, C.P. 2000. An Energy-Based Excess Pore Pressure Generation Model for Cohesionless Soils. Proceedings of the John Booker Memorial Symposium, 1–9.
- Ishihara K. 1985. Stability of natural deposits during earthquakes. Proceedings 11th International Conference on Soil Mechanics and Foundation Engineering, 321–276. <a href="https://doi.org/10.1007/978-3-319-73568-9">https://doi.org/10.1007/978-3-319-73568-9</a> 174
- Ishihara, K. 1996. Soil behaviour during earthquakes. Oxford engineering science series, Clarendon Press, Oxford, ISSN 0953-3222.
- Kokusho T. 2017. Liquefaction potential evaluations by energy-based method and stress-based method for various ground motions: Supplement. Soil Dynamics and Earthquake Engineering 95, April 2017, 40–47, https://doi.org/10.1016/j.soildyn.2017.01.033
- Kokusho T., and Mimori Y. (2015). Liquefaction potential evaluations by energy-based method and stress-based method for various ground motions. Soil Dynamics and Earthquake Engineering 75, 130–146. DOI:10.1016/j.soildyn.2015.04.002
- Kokusho T., and Kaneko Y. 2018. "Energy evaluation for liquefaction induced strain of loose sands by harmonic and irregular loading tests." Soil Dynamics and Earthquake Engineering 114, 362–377. DOI:10.1016/j.soildyn.2018.07.012.
- Lasley S.J., Green R.A., Chen Q.S., and Rodriguez-Marek A. (2016). Approach for Estimating Seismic Compression Using Site Response Analyses. ASCE *J. of Geotechnical and Geoenvironmental Eng.* 142(6), DOI:10.1061/%28ASCE%29GT.1943-5606.0001478
- Lasley S.J. (2015). Application of fatigue theories to seismic compression estimation and the evaluation of liquefaction potential. Ph.D. Dissertation, Virginia Tech, Blacksbrug, Virginia.

Proceedings of the 17<sup>th</sup> Pan-American Conference on Soil Mechanics and Geotechnical Engineering (XVII PCSMGE), and 2<sup>nd</sup> Latin-American Regional Conference of the International Association for Engineering Geology and the Environment (IAEG), La Serena Chile, 2024.

- Liang L. 1995. Development of an Energy Method for Evaluating the Liquefaction Potential of a Soil Deposit. Ph.D. dissertation. Case Western Reserve University, Cleveland, Ohio. 281p.
- NASEM (National Academies of Sciences, Engineering, and Medicine) 2016. State of the Art and Practice in the Assessment of Earthquake-Induced Soil Liquefaction and Its Consequences. Washington, DC: The National Academies Press. DOI:10.17226/23474
- Nemat-Nasser S., and Shokooh A. 1979. A unified approach to densification and liquefaction of cohesionless sand in cyclic shearing. *Canadian Geotechnical Journal* 16, 659–678.
- Polito C.P., Green R. A., Dillon E., & Sohn C. 2013. Effect of load shape on relationship between dissipated energy and residual excess pore pressure generation in cyclic triaxial tests. *Canadian Geotechnical Journal* 24, Sept 2013. https://doi.org/10.1139/cgj-2012-0379
- Polito C.P., Green R.A., and Lee J. 2008. Pore pressure generation models for sands and silty soils subjected to cyclic loading. ASCE J. of Geotechnical and Geoenvironmental Engineering 134(10),1490–1500.
- Poulos S.J., Castro G., and France J.W., 1985. Liquefaction evaluation procedure. ASCE J. of Geotechnical Engineering 111(6):772-792.
- Schofield A. and Wroth P. 1968. Critical State Soil Mechanics. McGraw-Hill Book Co., 310 p.
- Stark T.D., Olson S.M., Kramer S.L., and Youd T.L. 1999. Shear strength of liquefied soil. ASCE Geotechnical Special Publication 1(75), 313– 324
- Wu J., Kammerer A.M., Riemer M.F., Seed R.B. and Pestana J.M. 2004. Laboratory study of liquefaction triggering criteria. *Proceed 13<sup>th</sup> World Conference of Earthquake Eng.*, Vancouver, Paper No. 2580, 14 p.
- Yanagisawa E., and Sugano T. 1994. Undrained shear behaviors of sand in view of shear work. Proceed. 13th International Conference on Soil Mechanics and Foundation Eng., 5–10 January, New Delhi, 155–158.
- Yoshimine M., and Ishihara K. 1998. Flow potential of sand during liquefaction. Soils and Foundations 38(3), 189–198.
- Zavala G.J., Pando M.A., Park Y., and Aguilar R. (2022a) Specific Dissipated Energy as a Failure Predictor for Uniform Sands under Constant Volume Cyclic Simple Shear Loading. KSCE Journal of Civil Engineering. DOI 10.1007/s12205-021-1205-4
- Zavala G.J., Pando M.A., Park Y. and Aguilar R. (2022b). A simplified method for predicting failure of sands under general cyclic simple shear loading. *Geotechnical Research* 9(3), 141–154, <a href="https://doi.org/10.1680/jgere.22.00011">https://doi.org/10.1680/jgere.22.00011</a>

# INTERNATIONAL SOCIETY FOR SOIL MECHANICS AND GEOTECHNICAL ENGINEERING



This paper was downloaded from the Online Library of the International Society for Soil Mechanics and Geotechnical Engineering (ISSMGE). The library is available here:

# https://www.issmge.org/publications/online-library

This is an open-access database that archives thousands of papers published under the Auspices of the ISSMGE and maintained by the Innovation and Development Committee of ISSMGE.

The paper was published in the proceedings of the 17th Pan-American Conference on Soil Mechanics and Geotechnical Engineering (XVII PCSMGE) and was edited by Gonzalo Montalva, Daniel Pollak, Claudio Roman and Luis Valenzuela. The conference was held from November 12<sup>th</sup> to November 16<sup>th</sup> 2024 in Chile.